ACS APPLIED MATERIALS & INTERFACES

Research Article

www.acsami.org

Roughening in Electronic Growth of Ag on Si(111)-(7×7) Surfaces

Arindam Pal,[†] J. C. Mahato,[‡] B. N. Dev,[‡] and D. K. Goswami*[,†,§]

[†]Department of Physics and [§]Center for Nanotechnology, Indian Institute of Technology Guwahati, Guwahati, 781039, India

[‡]Department of Materials Science, Indian Association for the Cultivation of Science, Jadavpur, Kolkata 700032, India

ABSTRACT: Roughening in the electronic growth of Ag films on Si(111)-(7×7) surfaces for a film thickness ranging from 1 to 30 monolayers is reported. Ag films exhibit the growth of flat-top plateaus of preferential heights due quantum electronic effect. We have observed roughening of the film growth due to instability with linear diffusion characterized by the $\ln(\theta)^{1/2}$ dependence of the local surface slope, where θ is the Ag coverage. The roughening of the surface morphology has been characterized by scaling exponents α, β and $1/z$, which are determined using scanning tunneling microscopy. Increased value of $\alpha = 0.67 \pm 0.04$ at the early stage of the electronic growth with two atomic layer height flat-top isolated Ag mounds to 0.77 ± 0.06 at the later stage of the growth when isolated mounds coalesce and form percolated structures maintaining preferential heights of an even number of atomic layers in the Ag mounds indicates the instability in the electronic growth. As a result, interface width W increases as a power law of coverage (θ), $W \sim \theta^{\beta}$, with growth exponent $\beta = 0.33 \pm 0.03$, and lateral correlation length ξ grows as $\xi \sim \theta^{1/z}$ with $1/z = 0.27 \pm 0.05$.

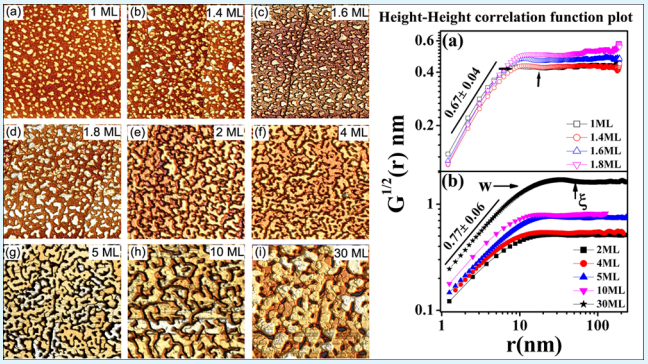

KEYWORDS: *electronic growth, roughening, Ag on Si, quantum well states, scaling exponents, local diffusion*

INTRODUCTION

Study of metal-semiconductor interfaces has been of great interest for decades in view of their technological applications. A large effort has been made to achieve the control of their electronic properties and to prepare the films with atomically flat surface morphology and interface, which are very important for microelectronic devices. In this regard, the Ag/Si(111) system is one of the most extensively studied because it is a nonreactive metal-semiconductor system.[1,2] Nevertheless, growth morphology of Ag film has been found to depend on the deposition rate and growth temperature.[3−5] Recently, "electronic growth" mode was proposed for growing a metal overlayer on semiconductor substrates. In the metal films, conduction electrons are confined by the metal surface at one side and the metal-semiconductor interface at other side. Due to this confinement, metal free electrons produce quantum well states (QWSs). However, the Ag film is stabilized due to the balance between energetic increase in quantum confinement and the decrease in the charge spill-out as thickness of the film increases.[6,7] As a result, a critical thickness of the film can be found beyond which smooth film can be grown.[8] The growth of Ag film on Si(111)-(7×7) surfaces has been found to follow the electronic growth. However, no critical thickness was reported from smooth film grown at room temperature (RT). In a novel two-step growth with deposition at low temperature (LT) and subsequent annealing at RT, the formation of 3D plateau-like Ag islands with strongly preferred height of two atomic layers on a wetting layer has been observed.[9] The islands increase the number density and lateral extension with coverage with no change in height and eventually form a percolated network-type growth. Investigations of both two-step growth and one-step growth by direct deposition at RT in the same work have been reported.[10,11] In ref 10, a nearly atomically flat surface morphology has been observed for a thickness of 6.4 ML in the two-step growth. Recently, we have reported the RT growth of Ag on Si(111)-(7×7) surfaces over a wide range of film thickness. This shows the formation of plateau-like percolated Ag islands with an N-layer (N even) height preference. We have not observed any thickness window within which a smooth Ag film can be grown as predicted by electronic growth. Nevertheless, Ag films were found to become rougher while growing. In order to understand this roughening mechanism in the electronic growth of Ag, we have examined the roughness evolution of the Ag films during the growth and explored the origin of this roughening mechanism that competes with electronic growth and makes the film rough. An instability at RT due to nonequilibrium film growth with local diffusion was found to be the origin of this roughening. Our findings provide an evidence of competition between roughening due to the local diffusion process with the smoothing due to QWS formation in electronic growth.

Received: June 11, 2013
Accepted: September 9, 2013
Published: September 9, 2013

   dx.doi.org/10.1021/am402258q | *ACS Appl. Mater. Interfaces* 2013, 5, 9517−9521

EXPERIMENTAL SECTION

Ag growth and scanning tunneling microscopy (STM) measurements were performed in a custom-made molecular beam epitaxy (MBE) chamber coupled with an ultra high vacuum (UHV) variable temperature scanning tunneling microscope (VTSTM, Omicron). Base pressure in the growth chamber was 1×10^{-10} mbar. Samples cut from a P-doped n-type Si(111) wafer (oriented within ±0.5°) with resistivity of 10−20 Ω cm were introduced in the UHV chamber. Atomically clean, reconstructed Si(111)-(7×7) surfaces were prepared by degassing at about ∼600 °C for 12−14 h and then flashing briefly at ∼1250 °C to remove the native oxide layer. The substrates were then cooled down to room temperature (RT) and (7×7) surface reconstruction was observed by STM. Ag atoms were evaporated from a Knudsen cell made of pyrolytic boron nitride (PBN) and deposited on the Si(111)-(7×7) reconstructed surface, which was kept at RT. The deposition rate was 2 monolayers/min for all the samples. We have deposited 1, 1.4, 1.6, 1.8, 2, 4, 5, 10, 30 ML Ag on Si(111)-(7×7) reconstructed surfaces. Here we define 1 monolayer (ML) of Ag as equivalent to the nominal surface atomic density of Ag(111), 1.5×10^{15} atoms/cm^2. The chamber pressure increased to 5×10^{-10} mbar during deposition. Following deposition the samples were transferred to VTSTM chamber for morphology characterization.

RESULTS AND DISCUSSION

Figure 1 shows representative STM images of Ag films for the coverages of 1 to 30 ML. Plateau-like Ag mound formation on

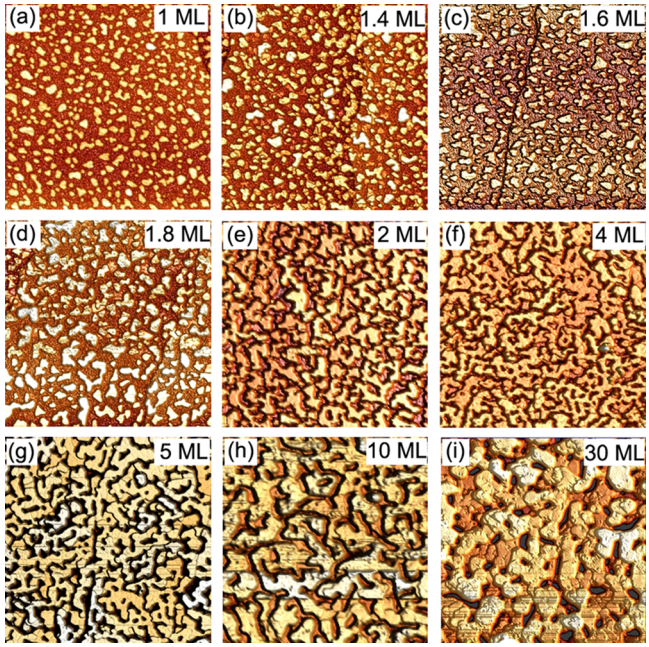

Figure 1. STM images of (a−i) Ag/Si(111)-(7×7) surfaces, showing the surface morphology for 1, 1.4, 1.6, 1.8, 2, 4, 5, 10, 30 ML coverage. All images represent a 500 × 500 nm^2 area.

top of a wetting layer is observed for the samples with Ag coverage of 1 to 1.8 ML (Figure 1a−d). These mounds have grown laterally with coverage, the height of the structures remaining constant. As Ag coverage increases, the mounds coalesce and from percolated structures. These mound structures grow vertically as well as laterally with Ag coverage ranging from 2 to 30 ML as shown in Figure 1e−i. A strongly preferred height of two atomic layers is observed for the samples up to 1.8 ML (below percolation). For thicker samples, percolated structures grow with the preference of N-layer height, where N is even (two, four, etc.) as reported in ref 11. This preferential height growth of Ag on Si(111)-(7×7) surfaces has been associated with electronic growth modes where electronic confinement within the metal film plays important role in determining the morphology of the films with magic heights, which are very often metastable.[9,11,12] The formation of such structures in two-step growth is recognized as the growth overcoming the kinetically limited diffusion processes. As a result, atomically smooth film growth may be possible. However, no smooth film growth is observed in single-step growth at RT even if preferred height growth is possible as predicted in electronic growth. However, a thick Ag film grown at RT and subsequently annealed at 700 °C does not show the formation of preferential height.[13]

In order to understand the dynamic behavior of the detailed growth processes, we have determined the different scaling exponents and local surface slope of the mounds. These quantities are determined from height−height correlation function, $G(r,\theta)$, which is defined as mean square of height difference between two surface positions separated by a distance r for coverage of the atom (θ) as $G(r,\theta) = \langle[h(r,\theta) - h(0,\theta)]^2\rangle$ where $h(r,\theta)$ and $h(0,\theta)$ are the heights of the surface at the locations separated by a distance r and the brackets signify an average over pairs of points.[14−17] As the growth rate of Ag is kept constant throughout the experiments, we have considered the dynamic behavior of the growth in terms of θ instead of time t. For the small r, height−height correlation function $G(r,\theta) = [m(\theta)r]^{2\alpha}$ with $r \ll \xi(\theta)$, where $\xi(\theta)$ is the characteristic in-plane length scale, α is the roughness scaling exponent, and $m(\theta)$ is the local slope of the surface profile for small length scale.[16,18] $m(\theta)$ is calculated from the fitting of linear portion of log−log plot of $G(r,\theta)$ vs r using the above equation. We have determined two parameters, which can be associated to describe mound growth. First one represents the average size of the mounds, whereas the second parameter represents average separation between mounds. Lateral correlation length, $\xi(\theta)$, is the measure of the length beyond which surface heights are not significantly correlated. For the mounded surfaces, this is essentially the size of the mounds.[19] The wavelength (λ), on the other hand, signifies the average separation between mounds. λ and ξ must satisfy the relation $\xi \leq \lambda$ because mounds are separated by at least their size. Only if the mounds grow next to each other would imply $\xi = \lambda$.[20] In case of percolated structures, λ is not well-defined. Therefore, we calculated ξ to characterize the Ag percolated mounds. Figure 2 shows the log−log variation of $G^{1/2}(r,\theta)$ vs r. To determine ξ, we have calculated $G(r,\theta)$ from STM images following the procedure described before. In order to avoid sampling induced effect in the $G(r,\theta)$ calculation, care has been taken to include many STM images in the averaging of $G(r,\theta)$ data. In our analysis we have checked that 6−10 STM images from each sample were enough to give statistically reliable data to obtain $G(r,\theta)$ plot. Figure 2a shows $G^{1/2}(r,\theta)$ vs r plots for the coverage up to 1.8 ML (below percolation), corresponding to the growth of mounds of two atomic layer preferred height. Figure 2b shows the same plot for the coverages ranging from 2 ML to 30 ML, when percolated Ag mounds were formed with preference of even atomic layers height. These mound structures grow vertically as well as laterally with coverage. However, we observed that the film becomes rougher with the growth. To monitor the roughening process quantitatively, we measure the interfacewidth $W(\theta)$ as function of θ. $W(\theta)$ (shown by arrow marked in Figure 2) is the value of $G^{1/2}(r,\theta)$ at the first local maximum, as $W(\theta) = G^{1/2}(\xi/2)$ where ξ,

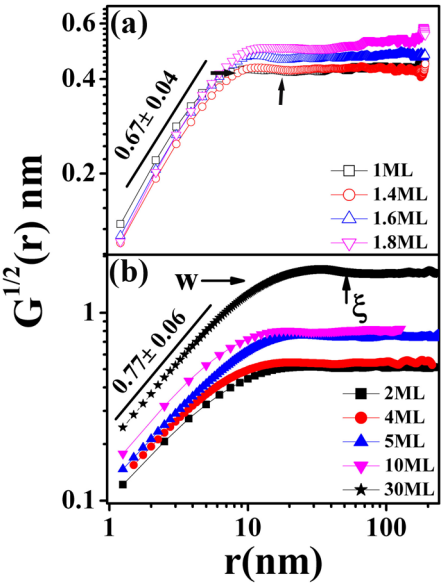

Figure 2. Square root of height−height correlation function calculated from STM images of (a) 1 to 1.8 ML Ag coverages and (b) 2 to 30 ML Ag coverages. Roughness exponent (α) is calculated from the power fitting of the linear portion.

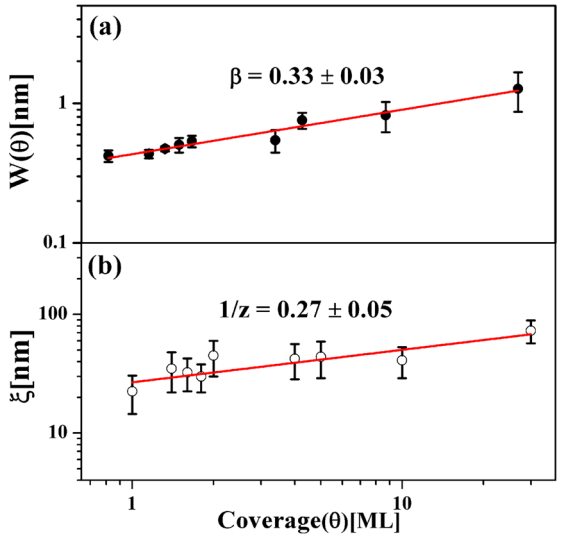

Figure 3. Log−log variation of (a) interface width (W) and (b) lateral correlation length (ξ) with coverages (θ). Growth exponent (β) and dynamic exponent ($1/z$) are calculated from the slope of the W and ξ curve, respectively.

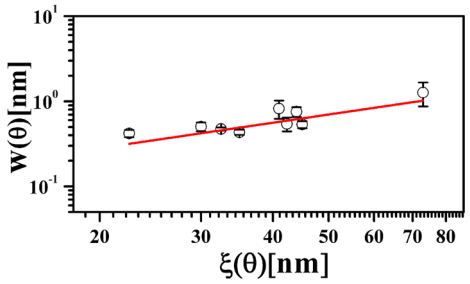

Figure 4. Log−log variation of interface width (W) with lateral correlation length (ξ). Solid curve represents the least-squares fit of the power equation to the data points.

marked by an upward arrow, is the position of r at the first local minimum of $G^{1/2}(r)$.[21] This definition of roughness amplitude is preferred over the large r limit of G (r) because artifacts at large length scales can affect STM data. The roughness exponent α was determined from a fit to the linear part of the log−log plot of $G^{1/2}(r)$ vs r. α essentially signifies the height fluctuation that corresponds to vertical growth of the film. We have observed two different values for α as shown in Figure 2; the two values are signifying two different growth regimes with coverages ranging from 1 to 1.8 ML and from 2 to 30 ML. In the first regime, Ag forms mounds with two atomic layer height preferences with $\alpha = 0.67 \pm 0.04$. In the second regime, α increases to 0.77 ± 0.06, and percolated Ag mounds with even atomic layer height preference are observed.

$W(\theta)$ increases following the power law as $W(\theta) \sim \theta^{\beta}$ with exponent $\beta = 0.33 \pm 0.03$. The exponent β characterizes the dynamics of the roughening process and is called growth exponent. The lateral correlation length $\xi(\theta)$ increases following the power law as $\xi(\theta) \sim \theta^{1/z}$, with $1/z = 0.27 \pm 0.05$. The exponent $1/z$ is called the dynamic exponent. Log−log variation of W and ξ versus θ are shown in Figure 3. Figure 3a shows the increasing nature of W as film grows. This clearly indicates the roughening of the film. However, the increasing nature of ξ with coverages, as shown in Figure 3b, confirms the lateral growth that makes the films smoother. Therefore, roughening and smoothening coexist and compete. However, we observed roughening in electronic growth. In order to quantify the dynamics of roughening, we have plotted ξ versus W for all the coverages. This is shown in Figure 4. From the equations of W versus θ and ξ versus θ, as described above, one can easily derive that $W = C\xi^{\beta/(1/z)}$, with the exponent $\beta/(1/z) = 0.99 \pm 0.11$, which is close to 1, and the constant C, which is 0.014 ± 0.008. In our case, the ratio of $\beta = 0.33 \pm 0.03$ and $1/z = 0.27 \pm 0.05$ is 1.22 ± 0.10, which is comparable with the fitted value within error bar. This essentially means the linear variation between W and ξ with slope ($dW/d\xi$) is 0.014. This slope estimates the competition between smoothing due to the lateral growth and roughening due to vertical growth. Smaller value of the slope indicates faster lateral growth than vertical growth, which essentially enables the smooth layer formation. Therefore, one can expect to have smooth film growth with a faster lateral growth process. As predicted in the electronic growth mode, the formation of discrete quantum well states can lead to novel effects including preferred heights and critical thickness of metal films beyond which the film will be atomically flat.[11,22−25] We have not observed any such critical thickness of Ag films grown on Si(111)-(7×7) surfaces. Faster lateral growth, as observed, can support the formation of smooth films. However, there is kinetic instability in the growth that does not allow the formation of smooth films, and a roughening in the growth mechanism is observed. A two-step growth mechanism has been popular in which films are grown at low temperature followed by room temperature annealing.[25,26] At low temperature, a nonequilibrium structure is formed, and this drives the system into a metastable state with height preference. However, it will not be accessible fully if unwanted kinetic processes are enabled. Room temperature growth of Ag films shows height preference as a consequence of "electronic growth" in which quantum well states can determine the film morphology, but kinetic processes cannot be suppressed completely. As a result, we observed roughening in the growth in terms of flat top mounds at the lower

dx.doi.org/10.1021/am402258q | ACS Appl. Mater. Interfaces 2013, 5, 9517−9521

coverages and percolated mounds at higher coverages with magic heights. This morphology is, essentially, due to the competition between quantum well state formation and kinetic growth processes.

From the theoretical treatments of nonequilibrium film growth, the predicted scaling exponents are $\alpha = 2/3$ and $\beta = 1/5$ if one considers the nonlinear growth equation.[27] However, the linear growth equation predicts $\alpha = 1$ and $\beta = 1/4$.[28] On the other hand, due to the step edge barrier (Schwoebel barrier), the diffusion can also be limited and form uniformly sized pyramids with stationary slope. The predicted scaling exponents for the Schwoebel barrier are $\alpha = 1$ and $\beta = 1/4$.[29] Actually, an understanding for the kinetic roughening in film growth is still far from complete.[30] None of these theoretical models support the exponents that we observed for electronic growth mode. In order to identify this roughening mechanism, we calculated local slope $m(\theta)$. If $m(\theta)$ is independent of the coverage (i.e., $m(t)$ is independent of time t), then it is said to be stationary. In such cases, height−height correlation function coincides for $r \ll \xi$. On the other hand, for nonstationary growth the local slope $m(\theta)$ increases with time and an upshift of $G(r,\theta)$ is observed as film thickness increases.[18] This represents mound growth. In nonequilibrium film growth driven by surface diffusion, the growth equation can be written as[31]

$$\frac{\partial h}{\partial t} = -\kappa\nabla^4 h + \lambda\nabla^2(\nabla h)^2 + F + \eta(r, \theta)$$

where κ and λ are constants, and η is a random fluctuation around the average flux F causing roughening. The linear and nonlinear parts determined by the constants κ and λ in the above equation represents the detail growth processes. Linear equation corresponds to the local growth when atoms sticks to the nearest kink sites irreversibly. A surface atom able to break the bonds and hop to the next sites represents the intermediate diffusion, and the growth processes are described by the nonlinear equation.[30] In case of local diffusion, the local surface slope increases with time and can be described as $m(\theta) = \langle(\nabla h)^2\rangle^{1/2} = (K \ln(\theta/\theta_c))^{1/2}$, where K is constant and θ_c is transition coverage to the scaling regime.[30,32] Figure 5 shows

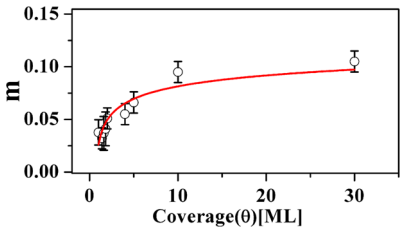

Figure 5. Plot of local slope $m(\theta)$ as a function of coverage (θ). The solid curve is a least-squares fit to the data points of $m(\theta) = (K \ln(\theta/\theta_c))^{1/2}$.

the plot $m(\theta)$ versus coverage (θ) and the fit with the equation described above. The value of θ_c obtained from the fit is 0.76 ML. This indicates that our smallest coverage sample (1 ML) is already into the scaling regime. This dependency is consistent with the local surface diffusion, which apparently causes the instability in the electronic growth in the single-step growth at RT. In our case, all samples were grown at room temperature. Therefore, the local surface diffusion at room temperature introduces instability in the electronic growth. As a result, the film becomes rough. Note that the continuum growth equation involves only height profiles h and it's derivatives, characteristic of the local nature of diffusion. However, the diffusion model only simply cannot explain the growth exponents that we observed. Electronic growth mechanism is also very significant to describe the film morphology evolution. Therefore, dynamic scaling behavior does not apply to our case. The observation of two roughness exponents ($\alpha = 0.67$ and 0.77) signifies growth below and above the percolation threshold. The growth is essentially lateral below the percolation threshold, keeping the bilayer height of the mounds constant. However, the percolated structures grow both vertically as well as horizontally, keeping the even atomic layer height preference. Therefore, the roughening behavior, observed in case of Ag growth at RT, belongs to a different universality class involving quantum well state formation along with local surface diffusion.

CONCLUSION

In conclusions, we report the origin of roughening in electronic growth of Ag film on Si(111)-(7×7) surfaces at room temperature. The film morphology is apparently influenced by the quantum well state formed within the films. However, we have found a roughening mechanism that exists with the electronic growth to control the surface morphology. This is due to local surface diffusion of the atoms at room temperature. The roughening behavior observed in the present study appears to belong to a different universality class, where electronic growth mechanism plays an important role.

AUTHOR INFORMATION

Corresponding Author

*E-mail: dkg@iitg.ernet.in.

Notes

The authors declare no competing financial interest.

REFERENCES

(1) Schmidt, W. G.; Bechstedt, F.; Srivastava, G. P. *Surf. Sci. Rep.* **1996**, *25*, 141−223.
(2) Vanloenen, E. J.; Iwami, M.; Tromp, R. M.; Vanderveen, J. F. *Surf. Sci.* **1984**, *137*, 1−22.
(3) Zhang, Z. H.; Hasegawa, S.; Ino, S. *Phys. Rev. B* **1997**, *55*, 9983−9989.
(4) Roos, K. R.; Tringides, M. C. *Surf. Sci.* **1994**, *302*, 37−48.
(5) Meyer, G.; Rieder, K. H. *Appl. Phys. Lett.* **1994**, *64*, 3560−3562.
(6) Tang, S. J.; Lee, C. Y.; Huang, C. C.; Chang, T. R.; Cheng, C. M.; Tsuei, K. D.; Jeng, H. T.; Yeh, V.; Chiang, T. C. *Phys. Rev. Lett.* **2011**, *107*, 066802−066805.
(7) Zhang, Z. Y.; Niu, Q.; Shih, C. K. *Phys. Rev. Lett.* **1998**, *80*, 5381−5384.
(8) Yu, H. B.; Jiang, C. S.; Ebert, P.; Wang, X. D.; White, J. M.; Niu, Q.; Zhang, Z. Y.; Shih, C. K. *Phys. Rev. Lett.* **2002**, *88*, 016102−4.
(9) Gavioli, L.; Kimberlin, K. R.; Tringides, M. C.; Wendelken, J. F.; Zhang, Z. Y. *Phys. Rev. Lett.* **1999**, *82*, 129−132.
(10) Hirayama, H. *Surf. Sci.* **2009**, *603*, 1492−1497.
(11) Goswami, D. K.; Bhattacharjee, K.; Satpati, B.; Roy, S.; Satyam, P. V.; Dev, B. N. *Surf. Sci.* **2007**, *601*, 603−608.
(12) Miyazaki, M.; Hirayama, H. *Surf. Sci.* **2008**, *602*, 276−282.
(13) Goswami, D. K. *Asian Journal of Physics* **2010**, *19*, 215−220.
(14) Barabási, A.-L.; Stanley, H. E. *Fractal Concepts in Surface Growth*; Cambridge University Press: Cambridge, 1995.
(15) Lapujoulade, J. *Surf. Sci. Rep.* **1994**, *20*, 191−249.
(16) Pelliccione, M.; Lu, T.-M. *Evolution of Thin Film Morphology: Modeling and Simulation*; Springer-Verlag: New York, 2008.
(17) Zhao, Y.; Wang, G.-C.; Lu, T.-M. *Characteriztion of Amorphus and Crystalline Rough Surface: Principles and Application*; Academic Press: London, 2001.

(18) Jeffries, J. H.; Zuo, J.-K.; Craig, M. M. *Phys. Rev. Lett.* **1996**, *76*, 4931−4934.
(19) Pelliccione, M.; Karabacak, T.; Gaire, C.; Wang, G.-C.; Lu, T.-M. *Phys. Rev. B* **2006**, *74*, 125420−10.
(20) Zuo, J.-K.; Wendelken, J. F. *Phys. Rev. Lett.* **1997**, *78*, 2791−2794.
(21) Kim, J.; Cahill, D. G.; Averback, R. S. *Phys. Rev. B* **2003**, *67*, 045404−6.
(22) Tang, S. J.; Lee, C. Y.; Huang, C. C.; Chang, T. R.; Cheng, C. M.; Tsuei, K. D.; Jeng, H. T.; Yeh, V.; Chiang, T. C. *Phys. Rev. Lett.* **2011**, *107*, 066802−5.
(23) Liu, H.; Zhang, Y. F.; Wang, D. Y.; Pan, M. H.; Jia, J. F.; Xue, Q. K. *Surf. Sci.* **2004**, *571*, 5−11.
(24) Huang, L.; Chey, S. J.; Weaver, J. H. *Surf. Sci.* **1998**, *416*, L1101−L1106.
(25) Smith, A. R.; Chao, K. J.; Niu, Q.; Shih, C. K. *Science* **1996**, *273*, 226−228.
(26) Neuhold, G.; Bartels, L.; Paggel, J. J.; Horn, K. *Surf. Sci.* **1997**, *376*, 1−12.
(27) Lai, Z.; Das Sarma, S. *Phys. Rev. Lett.* **1991**, *66*, 2348−2351.
(28) Wolf, D. E.; Villain, J. *Europhys. Lett.* **1990**, *13*, 389−394.
(29) Siegert, M.; Plischke, M. *Phys. Rev. Lett.* **1994**, *73*, 1517−1520.
(30) Jeffries, J. H.; Zuo, J.; Craig, M. M. *Phys. Rev. Lett.* **1996**, *76*, 4931−4934.
(31) Lai, Z.; Das Sarma, S. *Phys. Rev. Lett.* **1991**, *66*, 2348−2351.
(32) Amar, J. G.; Lam, P. M.; Family, F. *Phys. Rev. E: Stat. Phys., Plasmas, Fluids, Relat. Interdiscip. Top.* **1993**, *47*, 3242−3245.